

Publication VI

Ville Pietilä and Mikko Möttönen. 2009. Creation of Dirac monopoles in spinor Bose-Einstein condensates. *Physical Review Letters*, volume 103, number 3, 030401, 4 pages.

© 2009 American Physical Society (APS)

Reprinted by permission of American Physical Society.



Creation of Dirac Monopoles in Spinor Bose-Einstein Condensates

Ville Pietilä^{1,2} and Mikko Möttönen^{1,2,3}

¹*Department of Applied Physics/COMP, Helsinki University of Technology, P.O. Box 5100, FI-02015 TKK, Finland*

²*Australian Research Council, Centre of Excellence for Quantum Computer Technology, The University of New South Wales, Sydney 2052, Australia*

³*Low Temperature Laboratory, Helsinki University of Technology, P.O. Box 3500, FI-02015 TKK, Finland*

(Received 18 March 2009; published 13 July 2009)

We demonstrate theoretically that, by using external magnetic fields, one can imprint pointlike topological defects on the spin texture of a dilute Bose-Einstein condensate. The symmetries of the condensate order parameter render this topological defect to be accompanied with a vortex filament corresponding to the Dirac string of a magnetic monopole. The vorticity in the condensate coincides with the magnetic field of a magnetic monopole, providing an ideal analogue to the monopole studied by Dirac.

DOI: 10.1103/PhysRevLett.103.030401

PACS numbers: 03.75.Lm, 03.75.Mn

The existence of particles with a nonzero magnetic charge, that is, magnetic monopoles, has far reaching implications for the laws of quantum mechanics, theories of elementary particles, and cosmology [1–3]. However, experimental evidence of magnetic monopoles as fundamental constituents of matter is still absent, and hence there is great incentive to search corresponding configurations in experimentally more tractable systems. Several aspects of monopoles have been investigated in the context of liquid crystals [4], the anomalous quantum-Hall effect [5], exotic spin systems [6], and topological insulators [7]. Yet, an experimental realization of a magnetic monopole as an emergent particle or any analogy of the Dirac monopole [1] is still lacking. One of the candidate systems has been superfluid ³He [8–11], but to date there are no direct experimental observations of such topological excitations.

Dilute Bose-Einstein condensates (BECs) of alkali atoms with a hyperfine spin degree of freedom combine magnetic and superfluid order and share many features with the superfluid ³He [11–14]. The order parameter describing such systems is typically invariant under global symmetries that form a non-Abelian group. Monopoles and other textures can occur if this symmetry is spontaneously broken. Alternatively, light-induced gauge potentials can provide a realization of a magnetic monopole [15,16]. In the simplest case of a spin-1 condensate, a variety of different topological defects such as monopoles [17], non-trivial textures [18], and, in particular, analogies to the Dirac monopole [19] have been investigated. In the related two-component condensates, Skyrmions have been widely studied [20]. An experimental realization of any of these topological states still remains a milestone in the field of cold atoms.

In this Letter, we consider a spin-1 BEC which in the absence of external magnetic fields has two phases: a ferromagnetic and an antiferromagnetic (polar) phase [13]. In the presence of a strong enough external magnetic field, the spin of the condensate aligns with the local field, and the condensate order parameter corresponds to the

ferromagnetic phase. By modifying the external field adiabatically, multi-quantum vortices can be imprinted into the condensate [21]. The method we employ here utilizes the same ideology in this respect, but due to the nontrivial three-dimensional structure of the magnetic field we are able to create a pointlike defect to the spin texture of the condensate giving rise to a vorticity equivalent to the magnetic field of a magnetic monopole.

Let us assume first that the hyperfine spin of the condensate aligns with an external magnetic field which is a combination of two quadrupole fields and a homogeneous bias field

$$\mathbf{B}(\mathbf{r}, t) = B'_1(x\hat{x} + y\hat{y}) + B'_2z\hat{z} + B_0(t)\hat{\mathbf{b}}, \quad (1)$$

where Maxwell's equations impose the condition $2B'_1 + B'_2 = 0$. The direction of the bias field is determined by the unit vector $\hat{\mathbf{b}}$. Such a combination of quadrupole fields is produced by, e.g., a crossing pair of Helmholtz coils, and it has recently been shown to generate knotlike textures in antiferromagnetic BECs [18]. The point where the external magnetic field vanishes is the center of a monopole defect in the spin texture $\mathcal{S} = \Psi^\dagger \mathcal{F} \Psi$, given by the condensate order parameter $\Psi = (\psi_1, \psi_0, \psi_{-1})^T$ and the spin-1 matrices $\mathcal{F} = (\mathcal{F}_x, \mathcal{F}_y, \mathcal{F}_z)$. This monopole can be characterized by the charge [19]

$$\mathcal{Q} = \frac{1}{8\pi} \int_{\Sigma} d^2\sigma_i \varepsilon_{ijk} \varepsilon_{abc} \hat{s}_a \partial_j \hat{s}_b \partial_k \hat{s}_c, \quad (2)$$

where $\hat{s} = \mathcal{S}/|\mathcal{S}|$, the integral is taken over a surface Σ enclosing the defect, and the Levi-Civita symbol is denoted by $\varepsilon_{\alpha\beta\gamma}$. For the magnetic field in Eq. (1), the charge of the spin texture becomes $\mathcal{Q} = \pm 1$. A schematic illustration of two possible textures is shown in Fig. 1.

For the ferromagnetic order parameter manifold, the second homotopy group is trivial, and isolated monopole defects are not allowed. Thus the monopole defect in the spin texture is associated with a vortex filament extending outwards from the monopole giving rise to a physical Dirac string [1,19]. Since the monopole is located at the zero of

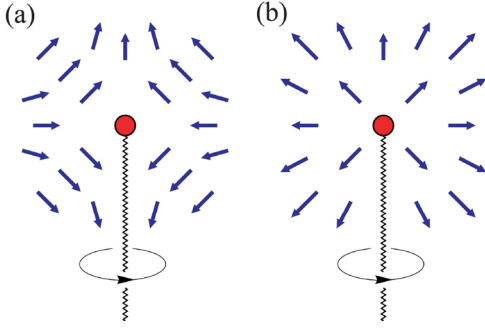


FIG. 1 (color online). Possible configurations for the spin texture. Both configurations are characterized by the same charge $Q = 1$, but only (a) can be imprinted using the quadrupole fields. The hedgehog texture (b) describes the vorticity $\mathbf{\Omega}_s$ corresponding to the spin texture in (a). In both cases, the vector fields are symmetric with respect to rotations about the axis on which the singularity filament (zigzag line) lies.

the magnetic field, adjusting the bias field $B_0(t)$ moves the monopole along the axis given by $\hat{\mathbf{b}}$. In particular, the monopole can be brought in from outside of the condensate by ramping down adiabatically an initially large bias field.

The superfluid velocity can be defined as $\mathbf{v}_s = -i\hbar\xi^\dagger\nabla\xi/m$, where $\Psi = \sqrt{\rho}\xi$, ρ is the density of particles, and m is the mass of the constituent atoms [13,19,22]. For simplicity, we first assume that $\hat{\mathbf{b}} = \hat{\mathbf{z}}$ and define new coordinates by $(x', y', z') = [x, y, 2z - B_0(t)/B'_1]$. In the adiabatic limit, the condensate order parameter corresponds to the local eigenstate of the linear Zeeman operator $g_F\mu_B\mathbf{B} \cdot \mathcal{F}$. Assuming that the local Zeeman energy is minimized for $B'_1 < 0$, $B_0 > 0$, and $g_F < 0$, we obtain in the $F = 1$ case

$$\mathbf{v}_s = \frac{\hbar}{m} \frac{1 - \cos\vartheta'}{r' \sin\vartheta'} \hat{\mathbf{e}}_{\varphi'}, \quad (3)$$

where $(r', \varphi', \vartheta')$ refer to spherical coordinates in the new coordinate system. A similar result has also been obtained in Ref. [19] for the hedgehog texture of Fig. 1(b).

The superfluid velocity \mathbf{v}_s is equivalent to the vector potential of a magnetic monopole and has a Dirac string along the negative z' axis if $B_0(t=0) > 0$. For spinor condensates the superfluid flow can be characterized by its vorticity $\mathbf{\Omega}_s = \nabla \times \mathbf{v}_s$, which becomes

$$\mathbf{\Omega}_s = \frac{\hbar}{m} \frac{1}{r'^2} \hat{\mathbf{e}}_{r'}, \quad (4)$$

indicating that vorticity corresponding to the imprinted monopole defect is equivalent to the magnetic field of a magnetic monopole; see Fig. 1. In particular, the topology of $\mathbf{\Omega}_s$ is unaffected by the scaling and translation, and hence $\mathbf{\Omega}_s$ remains equivalent to the hedgehog texture of Fig. 1(b) also in the original coordinate system. The Mermin-Ho relation for general spin F [22,23] yields

$$\mathbf{\Omega}_s = \frac{m_F\hbar}{2m} \varepsilon_{ijk} \hat{n}_i \nabla \hat{n}_j \times \nabla \hat{n}_k, \quad (5)$$

where $\hat{\mathbf{n}} = \mathbf{B}/|\mathbf{B}|$. In the adiabatic limit, spin \mathcal{S} aligns with $\hat{\mathbf{n}}$, and the charge Q in Eq. (2) is thus directly proportional to the flux of $\mathbf{\Omega}_s$ through a surface Σ enclosing the defect. The flux of the monopole is supplied by the Dirac string which is omitted from Eq. (4). In the case of $F = 1$, the monopole flux is $2\hbar/m$, that is, two angular momentum quanta, which implies that the vortex filament terminating at the monopole must carry the same amount of vorticity. The situation is thus similar to the Dirac monopole in superfluid $^3\text{He-A}$ [9,11]. For a general spin- F BEC, the Dirac string carries $2F$ quanta of angular momentum.

Nonadiabatic effects arising from interactions between atoms, kinetic energy, and the finite time scales in manipulating the external magnetic fields can render the spin to deviate from the direction of the local magnetic field. We take these effects into account by solving the dynamics of the spinor order parameter from the Gross-Pitaevskii (GP) mean-field equation [12,13]

$$i\hbar\partial_t\Psi = [\hat{h}_0 + c_0|\Psi|^2 + c_2(\Psi^\dagger\mathcal{F}\Psi) \cdot \mathcal{F}]\Psi, \quad (6)$$

where the interaction strengths c_0 and c_2 depend on the scattering lengths in the different channels corresponding to the total hyperfine spin of two scattering particles [13]. The single-particle operator \hat{h}_0 is given by $\hat{h}_0 = -\frac{\hbar^2}{2m}\nabla^2 + V_{\text{opt}} + g_F\mu_B\mathbf{B} \cdot \mathcal{F}$, where the optical potential is $V_{\text{opt}} = m r^2 \omega_r^2/2$ and we take other parameters according to ^{87}Rb implying ferromagnetic interactions.

In the simulation, energy, time, and spatial variables are given in the units of $\hbar\omega_r$, $1/\omega_r$, and $a_r = \sqrt{\hbar/m\omega_r}$, respectively. For $\omega_r = 2\pi \times 250$ Hz, the dimensional values of the parameters are given by $B'_1 = -0.05$ T/m and $B_0(t=0) = 1$ μT corresponding to 10^5 atoms. We have also considered a different atom number and antiferromagnetic interactions [24]. The volume considered in the simulation is $24 \times 24 \times 27$ in the units of a_r and the size of the computational grid varies from $141 \times 141 \times 161$ to $175 \times 175 \times 195$ points. In the simulation, we first calculate the ground state of the system corresponding to the initial values of the magnetic fields using the successive over relaxation algorithm and then propagate the initial state according to the time-dependent GP equation (6) using the split operator method combined with the Crank-Nicolson method. The time step used in the simulation is $10^{-4}/\omega_r$.

Since the Dirac string carries two quanta of angular momentum, it is expected to be prone to splitting into two separate strings each carrying one angular momentum quantum. To avoid this scenario, we first imprint the monopole defect with the bias field parallel to the z axis. The particle density from this simulation is shown in Fig. 2. The bias field is ramped linearly down to zero in a period $t_0 = 50/\omega_r$ and then equally to negative values. The spin texture \mathcal{S} takes the form of Fig. 1(a), and the corresponding vorticity is shown in Fig. 3(a). Since the monopole moves along the symmetry axis of the system, the Dirac string remains intact. The created monopole appears to be rela-

tively stable: After the bias field was ramped down, the monopole was allowed to evolve in time for a period $5/\omega_r$ in the presence of the two quadrupole fields resulting in slow small-amplitude oscillations along the z axis. Otherwise, the monopole remained intact. Because of non-adiabatic effects, the monopole defect in S lags slightly behind the zero point of the magnetic field and the Dirac string deviates from a pure δ -function distribution. For antiferromagnetic interactions [24], we obtained essentially the same behavior as in the case of ferromagnetic interactions.

If the rotation symmetry with respect to the z axis is explicitly broken by a bias field with $\hat{\mathbf{b}} \times \hat{\mathbf{z}} \neq 0$, we observe the Dirac string to split into two parts; see Fig. 3(b). The particle density is not depleted all of the way along the two strings suggesting that nonadiabatic effects become more pronounced. The spin density $|S|$, on the contrary, exhibits a clear depletion along the path of the two Dirac strings [26], and together with the state-of-the-art experimental methods [27,28] it should give an efficient signature of the monopole. In the experiments, a typical imperfection is a slight misalignment and slow drift between the center of the optical trap and the symmetry axis of the magnetic field. We model this by taking $\hat{\mathbf{b}} \parallel \hat{\mathbf{z}}$ and adding a small constant term $\tilde{B}_0 \hat{\mathbf{x}}$ to the magnetic field in Eq. (1). This introduces an offset equal to 7% of the effective radius of the condensate to the path traced by the monopole with respect to the z axis. The offset breaks the rotation symmetry of the system, but the Dirac string of this off-axis monopole remains undivided (data not shown) suggesting that the instability of the string becomes visible only for fairly large perturbations.

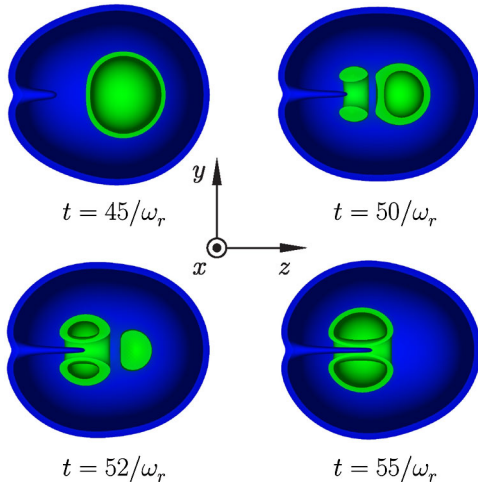


FIG. 2 (color online). Particle density at different stages of monopole creation. The monopole is created by ramping the bias field down in a period $t_0 = 50/\omega_r$. Blue (dark) color denotes densities from $\varrho = 3.8 \times 10^{-5} N/a_r^3$ to $\varrho = 1.8 \times 10^{-4} N/a_r^3$ and green (light) color densities from $\varrho = 1.4 \times 10^{-3} N/a_r^3$ to $\varrho = 1.5 \times 10^{-3} N/a_r^3$. The Dirac string is identified as the density depletion that propagates through the condensate.

Since the monopole defect in the spin texture is topologically unstable, it can be removed by local surgery. Thus we consider the dynamics of the monopole after the magnetic fields pinning the monopole are turned off. We have carried out simulations in which the external magnetic fields are switched off immediately or ramped down with constant speed in a period t_1 . For the finite switch-off times, the decay of the monopole initiates already while the external fields are being ramped down. The initial state corresponds to $t_0 = 50/\omega_r$ in Fig. 2.

For ferromagnetic interactions, we have used $t_1 = 0$, $t_1 = 2.5/\omega_r$, and $t_1 = 5.0/\omega_r$. In all three cases, the qualitative features are the same, and they are shown schematically in Fig. 4 (see also [26]). For the monopole defect in the spin texture, the monopole unwinds itself along the Dirac string and results in a closed vortex ring; see Figs. 4(a)–4(d). In the course of unwinding, a cylindrical domain wall separating the expanding core of the Dirac string from the rest of the texture is formed. Depending on how fast the external fields are turned off, the domain wall is either directly pushed out of the condensate (slow turn-off) or contracted to another vortex ring which eventually drifts out of the condensate (rapid turnoff). The resulting vortex ring persists until the end of the simulation which in all three cases spans a period $10/\omega_r$. Unwinding of the monopole in the vorticity Ω_s is depicted in Figs. 4(e)–4(h). During the unwinding of the monopole, vorticity concentrated at the Dirac string diffuses outwards and tends to relax towards more uniformly distributed values.

For antiferromagnetic interactions, we have carried out a simulation with magnetic fields ramped down linearly in a period $t_1 = 2.5/\omega_r$. The results agree qualitatively with the ferromagnetic case, and the end configuration is again a vortex ring in the spin texture. Another vortex ring is generated at the boundary of the condensate, and it persists

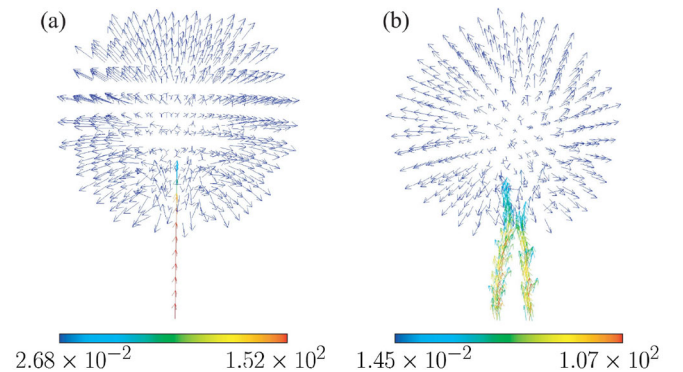


FIG. 3 (color online). Vorticity corresponding to the monopole. Vorticity Ω_s is computed numerically after the bias field is ramped from $B_0(0) = 1 \mu\text{T}$ to $B_0(t_0) = 0$, and it is shown in the units of h/ma_r . (a) $t_0 = 50/\omega_r$ and the bias field is parallel to the z axis. (b) $t_0 = 40/\omega_r$ and the bias field is parallel to the vector $3/2\hat{\mathbf{x}} + \hat{\mathbf{y}} + 14/3\hat{\mathbf{z}}$. The magnitude of the vorticity is denoted by color, and the map is linear between the minimum and maximum values. For clarity, only the relevant parts of the vector field Ω_s are shown.

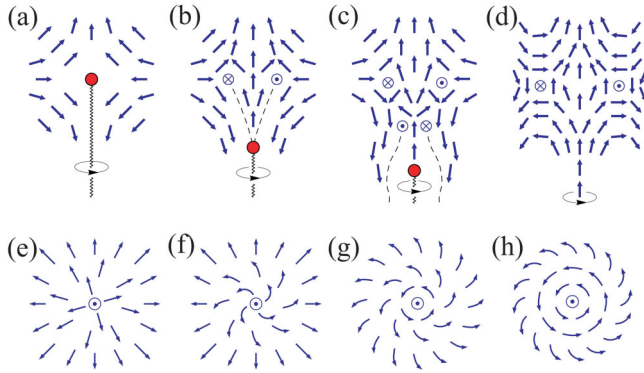


FIG. 4 (color online). Unwinding of the monopole defect in the spin texture S (a)–(d) and in the vorticity Ω_S (e)–(h). Arrows pointing upwards (downwards) from the plane are denoted by \odot (\otimes). Along the dashed line in (b) and (c), the spin points either upwards or downwards from the plane. The unwinding in Ω_S is shown in a plane perpendicular to the z axis, and it is qualitatively independent of the z coordinate. High-resolution figures from the simulation corresponding to these schematic illustrations are available in Ref. [26].

until the end of the simulation. The length of the simulation was $6/\omega_r$. We note that simulations concerning the unwinding of the monopole span a relatively short period, and it remains a question for future research to study whether the evolution of the created monopoles differs qualitatively between ferromagnetic and antiferromagnetic interactions. From the global symmetries of the order parameter in the absence of external fields [13,29], one could expect different behavior by purely topological reasoning [4]. Furthermore, we have not included the possible magnetic dipole-dipole interaction which may change the dynamics of the monopole unwinding. In particular, the spin texture in Fig. 1(a) resembles the so-called two- z -flare texture that was found to be stabilized by the dipole-dipole interaction [30].

In conclusion, we have introduced and modeled a robust method to create Dirac monopoles in spinor Bose-Einstein condensates. Using a tomographic reconstruction of the three-dimensional density profile [31], the Dirac string can be detected, and the corresponding spin texture can be explored using the *in situ* phase contrast imaging [27,28] providing an unambiguous signal of the monopole.

The authors acknowledge the Jenny and Antti Wihuri Foundation, the Emil Aaltonen Foundation, and the Academy of Finland for financial support and the Center for Scientific Computing Finland (CSC) for computing resources. We thank M. Krusius, G. Volovik, W.D. Phillips, and P. Cladé for discussions and J. Huhtamäki for help in numerical calculations.

- [1] P. A. M. Dirac, Proc. R. Soc. A **133**, 60 (1931).
- [2] A. Vilenkin and E. P. S. Shellard, *Cosmic Strings and Other Topological Defects* (Cambridge University Press, Cambridge, England, 1994).
- [3] A. H. Guth, Phys. Rev. D **23**, 347 (1981).
- [4] I. Chuang, R. Durrer, N. Turok, and B. Yurke, Science **251**, 1336 (1991).
- [5] Z. Fang *et al.*, Science **302**, 92 (2003).
- [6] C. Castelnovo, R. Moessner, and S. L. Sondhi, Nature (London) **451**, 42 (2008); L. D. C. Jaubert and P. C. W. Holdsworth, Nature Phys. **5**, 258 (2009).
- [7] X.-L. Qi *et al.*, Science **323**, 1184 (2009).
- [8] S. Blaha, Phys. Rev. Lett. **36**, 874 (1976).
- [9] G. E. Volovik and V. P. Mineev, JETP Lett. **23**, 593 (1976).
- [10] M. M. Salomaa, Nature (London) **326**, 367 (1987).
- [11] G. E. Volovik, *The Universe in a Helium Droplet* (Oxford University Press, Oxford, 2003).
- [12] T. Ohmi and K. Machida, J. Phys. Soc. Jpn. **67**, 1822 (1998).
- [13] T.-L. Ho, Phys. Rev. Lett. **81**, 742 (1998).
- [14] J. Stenger *et al.*, Nature (London) **396**, 345 (1998).
- [15] J. Ruseckas *et al.*, Phys. Rev. Lett. **95**, 010404 (2005); P. Zhang, Y. Li, and C. P. Sun, Eur. Phys. J. D **36**, 229 (2005).
- [16] V. Pietilä and M. Möttönen Phys. Rev. Lett. **102**, 080403 (2009).
- [17] H. T. C. Stoof, E. Vliegen, and U. Al Khawaja, Phys. Rev. Lett. **87**, 120407 (2001); J.-P. Martikainen, A. Collin, and K.-A. Suominen, Phys. Rev. Lett. **88**, 090404 (2002).
- [18] Y. Kawaguchi, M. Nitta, and M. Ueda, Phys. Rev. Lett. **100**, 180403 (2008).
- [19] C. M. Savage and J. Ruostekoski, Phys. Rev. A **68**, 043604 (2003).
- [20] J. Ruostekoski and J. R. Anglin, Phys. Rev. Lett. **86**, 3934 (2001); U. Al Khawaja and H. Stoof, Nature (London) **411**, 918 (2001); R. A. Battye, N. R. Cooper, and P. M. Sutcliffe, Phys. Rev. Lett. **88**, 080401 (2002); C. M. Savage and J. Ruostekoski, Phys. Rev. Lett. **91**, 010403 (2003).
- [21] M. Nakahara *et al.*, Physica (Amsterdam) **284B**, 17 (2000); T. Isoshima *et al.*, Phys. Rev. A **61**, 063610 (2000); S.-I. Ogawa *et al.*, Phys. Rev. A **66**, 013617 (2002); A. E. Leanhardt *et al.*, Phys. Rev. Lett. **89**, 190403 (2002); **90**, 140403 (2003).
- [22] T. L. Ho and V. B. Shenoy, Phys. Rev. Lett. **77**, 2595 (1996).
- [23] A. Lamacraft, Phys. Rev. A **77**, 063622 (2008).
- [24] For ^{87}Rb we have obtained a similar result for $N = 5 \times 10^4$ atoms. In the case of antiferromagnetic interactions, parameters were taken according to ^{23}Na corresponding to $B'_1 = -0.03$ T/m, $B_0(t=0) = 1$ μT , and $N = 4 \times 10^5$. The field gradients in the antiferromagnetic case should be large enough to exclude the ground state corresponding fragmented condensate; see Ref. [25].
- [25] T.-L. Ho and S. K. Yip, Phys. Rev. Lett. **84**, 4031 (2000).
- [26] See EPAPS Document No. E-PRLTAO-103-049930 for high-resolution figures. For more information on EPAPS, see <http://www.aip.org/pubservs/epaps.html>.
- [27] J. M. Higbie *et al.*, Phys. Rev. Lett. **95**, 050401 (2005).
- [28] L. E. Sadler *et al.*, Nature (London) **443**, 312 (2006).
- [29] F. Zhou, Phys. Rev. Lett. **87**, 080401 (2001).
- [30] M. Takahashi *et al.*, Phys. Rev. Lett. **98**, 260403 (2007).
- [31] R. Ozeri *et al.*, Phys. Rev. Lett. **88**, 220401 (2002).